Compact low loss and broadband hybrid plasmonic directional coupler

M. Z. Alam,* J. Niklas Caspers, J. S. Aitchison, and M. Mojahedi

Department of Electrical and Computer Engineering University of Toronto, 10 King's College Rd.,Toronto, Ontario M5S 3G4, Canada

**muhammad.alam@mail.utoronto.ca*

Abstract: We propose a novel broadband coupler for silicon photonics using a hybrid plasmonic waveguide section. The hybrid plasmonic waveguide is used to create an asymmetric section in the middle of a silicon nanowire waveguide coupler to introduce a phase delay to allow for a 3-dB power coupling ratio over a 150 nm bandwidth around 1.55 μm. The device is very compact (<8.5 μm) and has a low insertion loss (<0.15 dB).

OCIS codes: (130.3120) Integrated optics devices; (240.6680) Surface plasmons.

References and links

1. M. Davanço, P. Holmström, D. J. Blumenthal, and L. Thylén, "Directional coupler wavelength filters based on waveguides exhibiting electromagnetically induced transparency," IEEE J. Quantum Electron. **39**(4), 608–613 (2003).
2. C. K. Kirendall and A. Dandridge, "Overview of high performance fiber-optic sensing," J. Phys. D: All. Phys. **37**(18), R197–R216 (2004).
3. F. Aurzada, M. Scheutzow, M. Reisslein, N. Ghazisaidi, and M. Maier, "Capacity and delay analysis of next-generation passive optical networks (NG-PONs)," IEEE Trans. Commun. **59**(5), 1378–1388 (2011).
4. A. Takagi, K. Jinguji, and M. Kawachi, "Design and fabrication of broad-band silica-based optical waveguide couplers with asymmetric structure," IEEE J. Quantum Electron. **28**(4), 848–855 (1992).
5. L. Cao, A. Elshaari, A. Aboketaf, and S. Preble, "Adiabatic couplers in SOI waveguides," CLEO, paper CThAA2 (2011).
6. R. Halir, A. M. Novo, A. O. Monux, M. Fernandez, J. G. W. Perez, P. Cheben, D. X. Xu, J. H. Schmid, and S. Janz, "Colorless directional coupler with dispersion engineered sib-wavelength structure," Opt. Express **20**, 13470–13477 (2012).
7. S.-H. Hsu, "Signal power tapped with low polarization dependence and insensitive wavelength on silicon-on-insulator platforms," JOSA B. **27**(5), 941–947 (2010).
8. A. Takagi, K. Jinguji, and M. Kawachi, "Design and fabrication of broad-band silica-based optical waveguide couplers with asymetric structure," IEEE J. Quantum Electron. **28**(4), 848–855 (1992).
9. B. Chen, H. Lu, D. Zhao, Y. Yuan, and M. Iso, "Optimized design of polarization-independent and temperature-insensitive broadband optical waveguide coupler by use of fluorinated polyimide," Appl. Opt. **42**(20), 4196–4201 (2003).
10. M. Z. Alam, J. Meier, J. S. Aitchison, and M. Mojahedi, "Supermode propagation in low index medium," CLEO (2007) paper JThD112 (2007).
11. M. Z. Alam, J. Meier, J. S. Aitchison, and M. Mojahedi, "Propagation characteristics of hybrid modes supported by metal-low-high index waveguides and bends," Opt. Express **18**(12), 12971–12979 (2010).
12. D. Dai and S. He, "A silicon-based hybrid plasmonic waveguide with a metal cap for a nano-scale light confinement," Opt. Express **17**(19), 16646–16653 (2009).
13. P. D. Flammer, J. M. Banks, T. E. Furtak, C. G. Durfee, R. E. Hollingsworth, and R. T. Collins, "Hybrid plasmon/dielectric waveguide for integrated silicon-on-insulator optical elements," Opt. Express **18**(20), 21013–21023 (2010).
14. X. Sun, M. Z. Alam, S. J. Wagner, J. S. Aitchison, and M. Mojahedi, "Experimental demonstration of a hybrid plasmonic TE-pass polarizer for silicon-on-insulator platform," Opt. Lett. **37**, 4814–4816 (2012).
15. J. N. Caspers, M. Z. Alam, and M. Mojahedi, "Compact hybrid plasmonic polarization rotator," Opt. Lett. **37**(22), 4615–4616 (2012).
16. F. F. Lu, T. Li, X. P. Hu, Q. Q. Cheng, S. N. Zhu, and Y. Y. Zhu, "Efficient second-harmonic generation in nonlinear plasmonic waveguide," Opt. Lett. **36**(17), 3371–3373 (2011).
17. J. Wang, X. Guan, Y. He, Y. Shi, Z. Wang, S. He, P. Holmström, L. Wosinski, L. Thylen, and D. Dai, "Sub-μm2 power splitters by using silicon hybrid plasmonic waveguides," Opt. Express **19**(2), 838–847 (2011).

#187038 - $15.00 USD Received 11 Apr 2013; revised 11 Jun 2013; accepted 13 Jun 2013; published 27 Jun 2013

18. H.-S. Chu, Y. A. Akimov, P. Bai, and E.-P. Li, "Hybrid dielectric-loaded plasmonic waveguide and wavelength selective components for efficiently controlling light at subwavelength scale," J. Opt. Soc. Am. B **28** (12), 2895–2901 (2011).
19. B. E. A. Saleh and M. C. Teich, *Fundamentals of Photonics* (Wiley, New York, 2007).
20. E. D. Palik, *Handbook of optical constants of solids*, (Academic Press, Inc. 1985).
21. P. B. Johnson and R. W. Christy, "Optical constants of noble metals," Phys. Rev. B **6**(12), 4370–4379 (1972).
22. FDTD Solutions Reference Guide, (Lumerical Solutions, 2012).
23. G. V. Eleftheriades, A. S. Omar, L. P. B. Katehi, and G. M. Rebeiz, "Some important properties of waveguide junction generalized scattering matrices in the context of the mode matching technique," IEEE Trans. Microw. Theory Tech. **42**(10), 1896–1903 (1994).
24. V. M. N. Passaro, F. Dell'Olio, B. Timotijevic, G. Z. Mashanovich, and G. T. Reed, "Polarization-insensitive directional couplers based on SOI wire waveguides," The Open Optics Journal **2**(1), 6–9 (2007).
25. http://www.nanofab.ualberta.ca/wp-content/uploads/2009/03/pecvd_process_control.pdf

1. Introduction

A directional coupler is a very important component for many applications in integrated optics ranging from optical communication systems to biosensing [1–3]. The simplest form of directional coupler consists of two identical waveguides separated by a small gap to allow for coupling between the waveguides. This simple design is however very sensitive to the wavelength of operation. Although this wavelength dependence can be used for implementing useful devices such as optical filters [1], it limits the usefulness of the directional coupler for many other applications where a broadband response is required, for example optical sensing [2] and passive optical networking [3]. The bandwidth of the directional coupler can be increased by making the coupler asymmetric [4], adiabatic [5], by using a grating [6], or by introducing a bend in one arm of the coupler [7–9]. These approaches significantly increase the length of the coupler (over several hundred microns) and most of these designs are for low index contrast systems e.g., glass or fluorinated ploymide [8, 9]. There have been only a few reports of SOI compatible broadband directional couplers [5–7].

Recently we have proposed a hybrid plasmonic waveguide (HPWG) that consists of a metal plane separated from a high index material by a low index spacer [10, 11]. The proposed guide offers a number of advantages: it is very compact and provides a better compromise between loss and confinement compared to purely plasmonic guides. Since our first proposal, many different HPWG structures have been analyzed [12, 13] and many applications of the HPWG have been suggested [14–18]. These devices can outperform previously reported SOI based devices.

Here we propose a compact, broadband directional coupler using the HPWG concept and analyze its performance using full wave numerical analysis methods. The coupler uses an asymmetric section with an HPWG to compensate for the spectral dependence of the coupling between two identical silicon waveguides by introducing a phase difference between the fields in the two waveguides. We will first discuss the details of the operation as well as a simplified design method based on transfer matrix in the next section. The details of the final design as well as the full wave simulation results are presented in Section 3. The high sensitivity to fabrication imperfection is a major limitation of directional couplers. A possible way to correct for this limitation in case of our device is discussed in section 4.

2. Using a phase delay section to create a broadband directional coupler

The power transfer ratio of a directional coupler depends on the ratio of field amplitude at the two inputs and their relative phase. This concept can be used to make a cascade of directional coupler wavelength insensitive. In this approach by tuning the length of the first coupler and the length of the phase delay line, one controls the input field amplitude and phase for the second coupler in such a way that it cancels out the wavelength dependence of the first coupler section [9]. In this work we use the asymmetric section as the phase delay line between the two couplers. As we will see in later sections, such a design allows us to achieve a very broadband response using a very short device length. A top view of the proposed

#187038 - $15.00 USD Received 11 Apr 2013; revised 11 Jun 2013; accepted 13 Jun 2013; published 27 Jun 2013

broadband directional coupler is shown in Fig. 1(a). The device consists of three sections: the first and third sections are symmetric directional couplers consisting of two identical silicon waveguides (Fig. 1(b)) and the middle section is an asymmetric section consisting of a silicon waveguide and a HPWG (Fig. 1(c)). The silicon waveguide cross section is constant throughout the device (340 × 340 nm^2). Our device is designed for the quasi-TM mode of the waveguide. All the results presented in this paper are for the structure shown in Fig. 1(a). To connect the directional coupler with other on chip devices, waveguide bends must be used at the input and output of the proposed coupler [6]. Because of the high confinement of silicon waveguide modes, the effect of the bend on the coupling ratio is not large even for small bend radius. For example, in case of 6 μm long input and output bends, the coupling ratio changes by less than 2% for our final design described in Section 3. By excluding the waveguide bends in our simulation, we achieve significant saving in time and use of computational resources without sacrificing accuracy. A good understanding of the HPWG mode characteristic is essential for design of the proposed coupler. Such an analysis has been reported in [11].

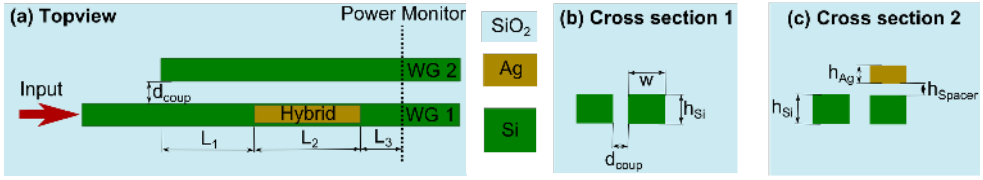

Fig. 1. (a) Top view of the broadband directional coupler (b) Cross section of the first and third silicon coupler sections. (c) Cross section of the second section. Positions of power monitors used in finite difference time domain (FDTD) simulation for calculating of power in the output waveguides are shown by dashed lines.

Figures 2 (a) and 2(b) show the mode profiles of the symmetric (+) and anti-symmetric (-) TM modes of the coupled silicon waveguides at 1.55 μm. The power coupling ratio of the directional coupler formed by the silicon waveguides depends on the amplitude and phase of the incident fields, and the difference in the propagation constants ($\Delta\beta = \beta_+ - \beta_-$) of the coupled modes [19]. This difference in propagation constant is wavelength dependent and thus the power transfer ratio of the silicon coupling section of Fig. 1(a) will be wavelength dependent (shown in Fig. 3, green line). To compensate the wavelength dependence of the power transfer ratio an asymmetric HPWG section is inserted between the symmetric sections. The HPWG inhibits coupling due to the large difference in both propagation constants and patterns of the TM silicon waveguide mode on the left and the TM hybrid waveguide mode on the right (Figs. 2(c), 2(d)). The difference in propagation constant of the non-coupling waveguides thus causes a wavelength dependent phase difference between the field coupled to WG 2 in section 1 and the field still in WG 1. Proper tuning of the lengths of the three sections allows for compensation of the wavelength dependence and leads to broadband operation.

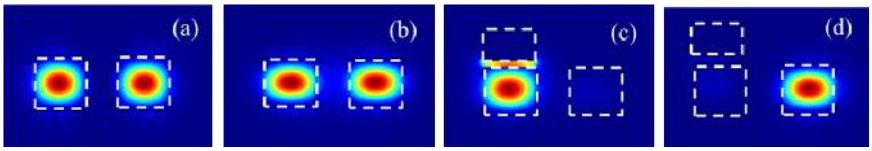

Fig. 2. Guided power density profiles of the TM modes of the directional coupler at 1.55 μm. (a) Even (b) odd supermodes in the silicon waveguide section. (c) and (d) even and odd modes in the asymmetric hybrid section. The boundaries between different layers are shown by dashed lines.

A simple transfer matrix model can be used to allow for a fast design process, where we calculated the field amplitude of the waveguide modes along our structure. The modes

#187038 - $15.00 USD Received 11 Apr 2013; revised 11 Jun 2013; accepted 13 Jun 2013; published 27 Jun 2013

supported by the cross-sections shown in Figs. 1(b) and 1(c) were calculated using a commercial finite element code (Comsol Multiphysics). The transmitted power was then calculated by propagating these modes along the sections and calculating the coupling between the modes by evaluating the power overlap.

$$\vec{a}_{Start} = \frac{1}{\sqrt{2}}\begin{pmatrix}1\\1\end{pmatrix};\ \ddot{P}_M = \begin{pmatrix} e^{i\beta_+^M L_M} & 0 \\ 0 & e^{i\beta_-^M L_M}\end{pmatrix};\ \ddot{T}_{12} = \begin{pmatrix} c_{11} & c_{12} \\ c_{21} & c_{22}\end{pmatrix} \quad (1)$$

$$\vec{a}_{End} = \ddot{P}_3 \cdot \ddot{T}_{12}{}^T \cdot \ddot{P}_2 \cdot \ddot{T}_{12} \cdot \ddot{P}_1 \cdot \vec{a}_{Start} \quad (2)$$

Here $\ddot{P}_M$ describes the propagation of the two modes present in section M, using the propagation constant $\beta_{+/-}$ and the length of the section L_M. The coupling between the sections is described using the transfer matrix $\ddot{T}_{12}$ with the coupling constants c_{ij} calculated using the integral over the power overlap of the modes involved. The final transmission can be found by multiplying the matrices for the three sections, where the elements of the final vector ($\vec{a}_{End} = \ddot{P}_3 \cdot \ddot{T}_{12}{}^T \cdot \ddot{P}_2 \cdot \ddot{T}_{12} \cdot \ddot{P}_1 \cdot \vec{a}_{Start}$) each give the field amplitude of the supermodes. The above mentioned design method significantly speeds up the design process of the broadband coupler.

3. Design of a 3 dB broadband HPWG coupler

Depending on the application different coupling ratios can be chosen. Here we present the design for a 3-dB coupler. To simplify the design process we used the simple transfer matrix based design method described in Section 2. The length of three sections as well as the thickness of the silica layer between the silicon and the gold in the hybrid section was varied to achieve broadband coupling. The final design was simulated using a three dimensional finite difference time domain code Lumerical to confirm the results obtained from the simplified design process. The material properties of silica and silicon are taken from [20] and that of gold is taken from [21]. The mesh accuracy and simulation size were varied to ensure convergence and to estimate the numerical error. Power at the two output waveguides are calculated by integrating the power density over the cross sections at the end of the waveguides marked by dashed lines in Fig. 1(a) by using two power monitors [22]. The final device dimensions for the 3 dB coupler design are w = 340 nm, h_{Si} = 340 nm, h_{spacer} = 45 nm, d_{coup} = 220 nm, L_1 = 4.5 μm, L_2 = 3 μm, L_3 = 0.8 μm. The power transfer ratio for the final design calculated using a full-wave three dimensional simulation FDTD simulation is shown in Fig. 3 (red line). Here power transfer ratio (η) is defined as $\eta = P_2/(P_1 + P_2)$; P_1 and P_2 are power outputs at first and second branches respectively. The power transfer ratio is close to 0.5 (with the value of η limited within the range 0.45 to 0.55) for the wavelength range 1.45 to 1.6 μm. For comparison the results obtained from the transfer matrix model is also shown (blue line). Both models show good agreement. The slight deviations are caused by reflections between the sections, which could be eliminated by implementing an Eigenmode expansion method (EME) instead of the transfer matrix model [23]. The insertion loss of the coupler is less than 0.2 dB over the entire range. Here insertion loss is defined as the power loss caused by the directional coupler when it is inserted between silicon waveguides having same cross sections (340 nm × 340 nm). This loss includes propagation loss caused by presence of metal and reflection loss at the two ends of the directional coupler. Since the HPWG section is very short, the presence of metal has very little effect on the insertion loss, and the overall insertion loss is negligible.

#187038 - $15.00 USD Received 11 Apr 2013; revised 11 Jun 2013; accepted 13 Jun 2013; published 27 Jun 2013

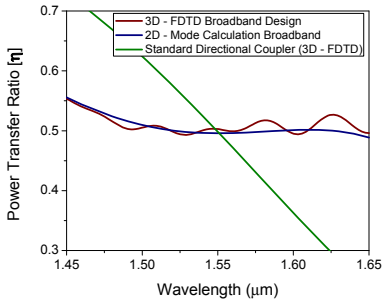

Fig. 3. Power transfer ratio for the broadband coupler calculated using full 3D FDTD (red) and the 2D approach (blue) as well as the coupling coefficient for a non-broadband coupler with the same waveguide dimensions (green).

4. Compensation for fabrication imperfections

Directional couplers are very sensitive to fabrication imperfections, especially in high contrast waveguide systems such as silicon photonics [24]. Figures 4(a) and 4(b) show the effects of varying waveguide width (w) and spacer height (h_{spacer}) from the design specifications, while all other dimensions and material properties are kept constant. We have also examined the effect of temperature variation on the device performance. Although silicon has a high thermo optic coefficient (1.8×10^{-4}/K) due to the short length, the proposed device is not very sensitive to temperature variations. For example, for 25°C temperature change, the coupling ratio changes by less than 0.03 dB.

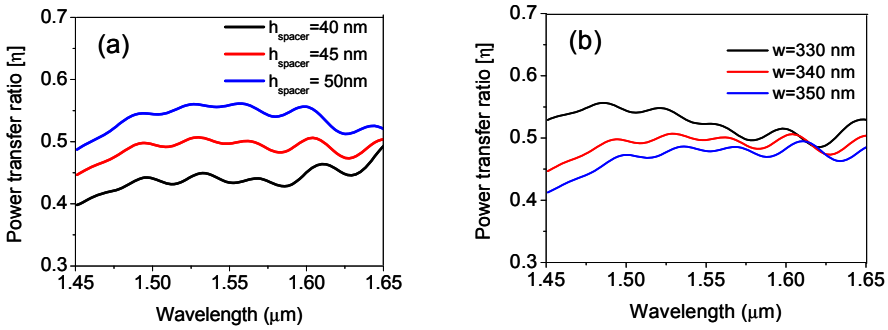

Fig. 4. Power transfer ratio of the broadband coupler when the dimensions are different from design specifications. (a) Effect of spacer height variation (b) Effect of waveguide width variation. All other dimensions are same as the final design described in section 3.

Since dielectric waveguide based directional couplers depend on a single etch step for their implementation, there is no straightforward way to correct for possible variation of width from design value which may occur during fabrication. Fabrication of the proposed device will require etching of silicon followed by either thermal oxidation or PECVD for depositing the spacer layer followed by a metal deposition and lift off [14]. If after the etching, it is found that the silicon waveguide widths are different from the design, the desired power transfer ratio over a broad wavelength range can still be obtained by changing the thickness of the spacer layer.

To illustrate this we have considered the scenario when the spacing between the waveguides for the final design (d_{coup}) changes from 220 nm from 250 nm. As shown by the dashed red line in Fig. 5, the device does not work as a 3 dB coupler after such a change. However, as shown by the solid black line of Fig. 5 by changing the spacer thickness to 65

#187038 - $15.00 USD Received 11 Apr 2013; revised 11 Jun 2013; accepted 13 Jun 2013; published 27 Jun 2013

nm and by changing the section lengths to L_1 = 4 μm, L_2 = 3.5 μm, L_3 = 0.8 μm, 3 dB operation of the device can be restored. Dielectric film thickness accuracy within a few nm can be readily achieved using standard fabrication processes, for example plasma enhanced chemical vapor deposition (PECVD) [25]. Although we have considered only one possible scenario, i.e., variation of waveguide spacing, the effects of other fabrication imperfections on the coupler performance, e.g., variation of waveguide width (w) or variations of both waveguide width (w) and gap (d_{coup}) can also be corrected in a similar manner. The proposed design, therefore, has the additional advantage to be able to compensate for fabrication imperfections and thus is more robust in terms of fabrication tolerance.

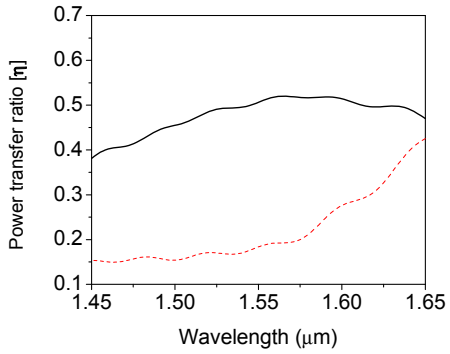

Fig. 5. Power transfer ratio of the broadband coupler when gap width is increased by 30 nm from final design (dashed line) and after the adjustment of metal section length and spacer thickness (solid line).

5. Conclusion

We have proposed a broadband directional coupler for silicon on insulator platform using the recently proposed HPWG. The device is very short, has low insertion loss and is wavelength insensitive over more than a 150 nm bandwidth with less than 5% variation of power transfer ratio. Performance of the device compares favorably against previously reported devices. Both adiabatic couplers [5] and directional coupler using a Mach-Zehnder interferometer [7] can offer a broadband response but require length exceeding several hundred micrometers. In contrast the proposed HPWG based directional coupler, while has a wavelength independent response over 150 nm bandwidth with an imbalance less than 5% and a length of less than 10 μm. The design presented in this work therefore, can be an important component for future silicon based optical communications systems.

#187038 - $15.00 USD Received 11 Apr 2013; revised 11 Jun 2013; accepted 13 Jun 2013; published 27 Jun 2013